Proceedings of the 17th Czech and Slovak Conference on Magnetism, Košice, Slovakia, June 3–7, 2019

Crystal Structure and Magnetocaloric Effect of $La_{0.80}Ag_{0.15}MnO_3$ Nanoparticles

M. Zentková[a,*], M. Mihalik[a], M. Mihalik Jr.[a], M. Kovalik[a], M. Perovic[b], M. Vavra[c] and J. Briančin[d]

[a]Institute of Experimental Physics SAS, Watsonova 47, 04001 Košice, Slovakia
[b]Institute of Nuclear Sciences Vinca, University of Belgrade, 11001 Belgrade, Republic of Serbia
[c]Faculty of Science,P.J. Šafárik University, Moyzesova 11, 04001 Košice, Slovakia
[d]Institute of Geotechnics SAS, Watsonova 45, 04001 Košice, Slovakia

Annealing of non stoichiometric $La_{0.80}Ag_{0.15}MnO_3$ nanoparticles leads to the change of the crystal symmetry from $Pnma$ to $R\bar{3}c$ and to almost doubling of its Curie temperature from 117 K to 317 K. This effect is due to the releasing of lattice distortions and strengthening of double exchange interaction. The large values of the magnetocaloric entropy of the order of $\Delta S = 6.19$ J/(kg K) were observedat $\Delta\mu_0 H = 5$ T and $T = 315$ K.

DOI: 10.12693/APhysPolA.137.900

PACS/topics: manganites, nanoparticles, magnetic properties, magnetocaloric effect

1. Introduction

Magnetic cooling based on magnetocaloric effect (MCE) is a simple, convenient, and more promising attractive cooling technology than the classical one used in the vapour compression refrigerators [1]. MCE is an intrinsic property for all magnetic materials. Materials exhibiting the large MCE are actively sought and investigated [2]. Large values of the MCE are observed in rare-earth elements [1, 2]. Perovskite lanthanum hole doped manganites with a general formula of $La_{1-x}Ag_xMnO_3$ have arisen as potential candidates in magnetic refrigeration at various temperature ranges [3–5]. Recently, it was shown on $La_{0.80}Ag_{0.15}MnO_3$ ceramic that the magnetic entropy change is 5.6 J/(kg K) for the field change of 2.6 T at 270 K, which corresponds to 6 J/(kg K) for Gd [3]. A significant advantage of these materials is the possibility of controlling the temperature of phase transitions in a wide range including room temperature, by varying the concentrations of the constituent chemical elements and conditions of synthesis [5, 6]. Nowadays, the interest shifts from classical ceramic materials [3–5] towards nanosized materials [7]. This work is continuation of our previous research of nanosized $La_{1-x}Ag_xMnO_3$ materials [8]. In our study we modify magnetic properties of $La_{0.80}Ag_{0.15}MnO_3$ nanosized off stoichiometric material by heat treatment in order to reach magnetic transition above the room temperature.

Nanosized powder $La_{0.80}Ag_{0.15}MnO_3$ was prepared by the glycine-nitrate method, which is advantageous due to series of simple steps and the ability to achieve greater efficiency compared to other methods [9].

2. Experimental procedure

A molar ratio between glycine and nitrate was equal 1. Formation of agglomerates was suppressed by additional oxidant $(NH_4)(NO_3)$, which was added to solution with the same weight as glycine. The as-prepared samples were afterwards annealed at 800 °C for 1, 12 and 48 hours in the air. We use labels $as0$, $1h$, $12h$ and $48h$ when refering to these four samples in the main text. Powder X-ray diffraction (XRPD) measurements at room temperature were carried out on the Rigaku Ultima IV diffractometer. The diffraction patterns were analyzed by the FullProf program that is based on the full-profile Rietveld method [10]. The basic parameters of crystal structure are summarised in Table I. The as-prepared sample adopts orthorhombic crystal structure ($Pnma$). The building blocks MnO_6 of the crystal structure were deformed by Jahn Teller (JT) distortion, and were tilted. We expected that the degree of JT distortion is large [11]. The annealed samples crystallized in rhombohedral structure ($R\bar{3}c$). The size of nanoparticles increased with annealing time, and then the amount of precipitated Ag was reduced. Scanning electron microscopy (SEM) was performed on Mira III FE (Tescan). The SEM analysis confirmed our previous results [8], namely that the prepared samples in the form of fine powder form agglomerates and the size of nanoparticles scales the size determined by XPRD (Table I). The mixed-valence state was determined with iodometric titration. The average oxidative state increased with heating due to incorporation of Ag into the lattice, and was close to 3.30. Such result implies the presence of 70% of Mn^{3+} and 30% of Mn^{4+} in samples.

*corresponding author; e-mail: zentkova@saske.sk

3. Results and dicussion

Magnetization and AC susceptibility measurements were done by the Quantum Design MPMS XL-5 SQUID magnetometer. Our measurements revealed that all samples undergo paramagnetic (PM) to ferromagnetic (FM) transition at the Curie temperature T_C. The examples of the temperature dependences of magnetization in zero field cooled (ZFC) and field cooled (FC) regimes and DC susceptibility are shown in Fig. 1. The hysteretic behaviour between magnetization measurements performed in ZFC and FC regimes for low applied magnetic fields is typical feature of all samples. Bifurcation temperature T_b is comparable with the Curie temperature T_C, which was determined as a minimum on $\mathrm{d}\mu/\mathrm{d}T(T)$ and $\mathrm{d}\chi'/\mathrm{d}T(T)$ dependence or from Arrot's plots. The value of T_C increases from 117 K for sample $as0$ to 310 K, 316 K and 317 K for annealed samples $1h$, $12h$ and $48h$, respectively, as shown in Fig. 1a. Doubling of T_C is mainly due to reduction of JT distortions and to the increase of bonding angle Mn–O–Mn induced by crystal structure transformation from $Pnma$ to $R\bar{3}c$ (Table I). It was shown theoretically that the JT coupling drastically reduces the Anderson-Hasegawa double exchange (DE) due to reduction of mobility of electrons, which is required by mechanism of this interaction [12]. XRPD measurements in analogy with our study performed on $La_{0.7}Ca_{0.3}MnO_3$ system of nanoparticles [11], indicate that the JT distortion of crystal lattice is enhanced on as-prepared sample. The pressure effect on T_C causes that due to very low mobility of $3d$ electrons the dominant exchange interaction in the case of as-prepared sample is superexchange [13, 14]. The releasing of JT distortion by the heat treatment leads to enhanced $T_C = 225$ K preserving $Pnma$ structure, as was shown for ceramic sample with stoichiometric composition $La_{0.85}Ag_{0.15}MnO_3$ [4]. Additional rise of T_C is attributed to the increase of bonding angle Mn–O–Mn due to the structure phase transformation, because the strength of (DE) ferromagnetic interactions and the corresponding value of T_C are proportional to a bandwidth of the conduction e_g electrons, given by $W = \nu \cos(\phi) \cos(\theta_{ij}/2)$, where ν is the covalent mixing parameter, ϕ is the bond-bending angle ($\phi = (180^\circ - \beta)$), β is Mn–O–Mn bond angle, and θ_{ij} is the angle between the two spin directions of the neighbouring manganese ions [15].

High temperature magnetic inverse susceptibility $1/\chi$ (insert of Fig. 1b) indicates the validity of the Curie-Weiss law, i.e., $\chi = C/(T - \theta)$, for all samples in temperature region enough high above T_C (C is the Curie constant, and θ is the paramagnetic Curie-Weiss temperature). Therefore, for $as0$, $1h$, $12h$ and $48h$ samples we have $\theta = 116$ K, 310 K, 318.4 K, and 318 K, and $\mu_{\mathrm{eff}} = 4.99\mu_B$, $\mu_{\mathrm{eff}} = 5.17\mu_B$, $\mu_{\mathrm{eff}} = 4.64\mu_B$, and $\mu_{\mathrm{eff}} = 5.32\mu_B$, respectively. The experimental values of μ_{eff} are very close, especially for sample $12h$, to theoretical predictions $\mu_{\mathrm{eff}} = 4.62\mu_B$. In fact, this assumes the presence of 70% of Mn^{3+} ($4.90\mu_B$) and 30% of Mn^{4+} ($3.87\mu_B$) in samples.

The transition from ferromagnetic (FM) to paramagnetic (PM) phase on rhombohedral sample $48h$ is accompanied by the presence of distinguished maxima in both in-phase $\chi'(T)$ at 301 K and out-of-phase $\chi''(T)$ at 305 K components of AC susceptibility (Fig. 2a). The temperature dependence of $\chi'(T)$ corresponds very well to measurements of magnetic moment in ZFC regime.

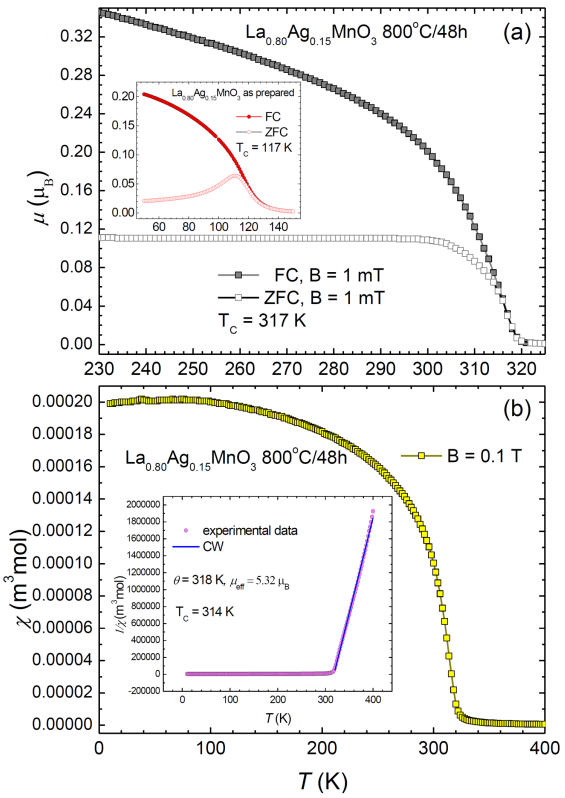

Fig. 1. Temperature dependence of (a) magnetization in ZFC and FC regimes for annealed sample $48h$ (and for sample $as0$ in insert), (b) susceptibility (and inverse susceptibility in insert) for annealed sample $48h$.

TABLE I

Summary of basic crystal parameters for as prepared sample and annealed samples at 800 °C

Sample	Crystal structure	a [Å]	b [Å]	c [Å]	V [Å^3]	Mn–O$_1$–Mn angle β_1 [°]	Mn–O$_2$–Mn angle β_2 [°]	Particle size [nm]	Ag content [%]	Oxidative state
$as0$	$Pnma$	5.5791	7.7615	5.5342	239.64	155.799	136.686	22.614	4.33	–
$1h$	$R\bar{3}c$	5.4986	5.4986	13.3596	349.81	165.518	–	36.740	0.22	–
$12h$	$R\bar{3}c$	5.4976	5.4976	13.3618	349.74	165.520	–	39.766	0.48	3.30
$48h$	$R\bar{3}c$	5.5001	5.5001	13.3604	350.02	165.517	–	48.099	0.33	–

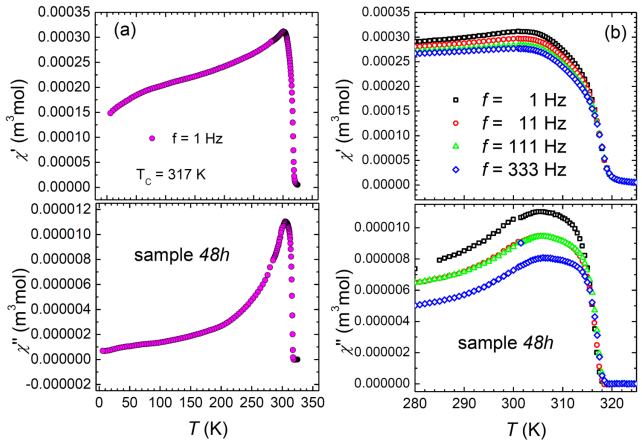

Fig. 2. Temperature dependence of (a) AC susceptibility in wide temperature range, and (b) frequency.

Change of slope in $\chi'(T)$ and a dull maximum in $\chi''(T)$, which start to develop below 55 K, can indicate a creation of short range antiferromagnetic correlations, or can be attributed to freezing of magnetic moments. The mentioned anomaly is weaker than in orthorhombic $La_{0.85}Ag_{0.15}MnO_3$ sample [4]. Figure 2b demonstrates frequency dependence of maxima in $\chi'(T)$ and $\chi''(T)$, which are reduced by the frequency increase, but do not change their position.

The ferromagnetic character of samples is evident from magnetic hysteresis loops taken at 5 K (Fig. 3a). The coercive force decreases from 156.65 mT for *as*0 to 16.2 mT for 48*h* with annealing (insert Fig. 3a), and for rhombohedral samples is negligible at room temperature. The magnetization of *as*0 sample does not completely saturate at 5 T, and both remnant and saturated magnetization increases with annealing.

Figure 3b shows a dependence of B/μ vs. μ^2, which is known as the Arrott plots for sample 48*h* which was constructed from magnetic isotherms in the vicinity of T_C. The positive slope in almost the whole temperature range indicates the second order magnetic transition. The same conclusion can be made from the Arrott plots constructed for *as*0 sample. The magnetocaloric properties of $La_{0.80}Ag_{0.15}MnO_3$ nanoparticles, orthorhombic sample *as*0 and rhombohedral sample 48*h*, have been investigated by indirect method based on determination of the magnetic entropy change ΔS from measurements of magnetic isotherms in a given temperature range. For sample *as*0 the range varies from 95 K to 170 K, and for sample 48*h* is was from 280 K to 345 K. The temperature dependence of $-\Delta S(T)$ in respect with applied magnetic field which is shown in Fig.4. The highest values $-\Delta S \approx 1.22$ J/(kg K) ($\Delta\mu_0 H = 5$ T) for *as*0 sample (*Pnma*) are typical for temperature range near T_C between 112 K and 123 K, which corresponds to very broad transition to ferromagnetic state. The determined value is much smaller than $-\Delta S = 5.16$ J/(kg K) ($\Delta\mu_0 H = 5$ T, $T = 270$ K) for

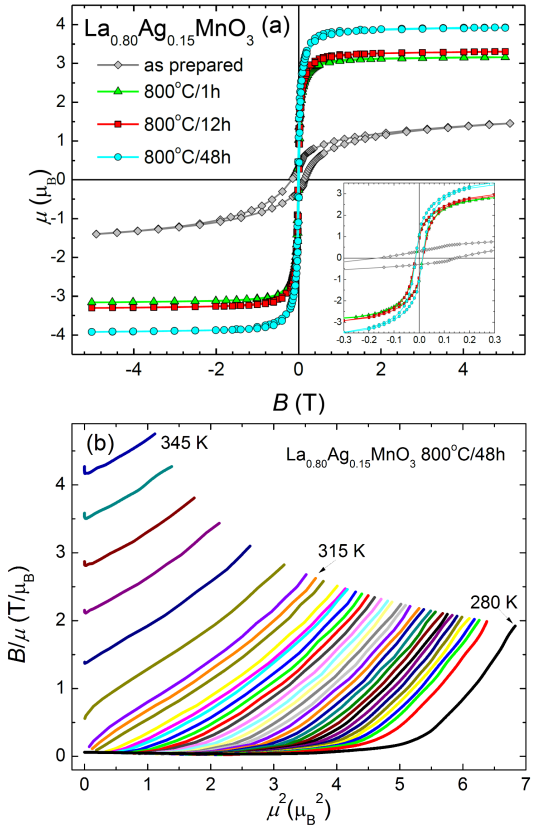

Fig. 3. (a) Magnetic hysteresis loops taken at 5 K. (b) Arrott plots for the isotherms of 48*h* sample in the temperature range from 280 K to 345 K.

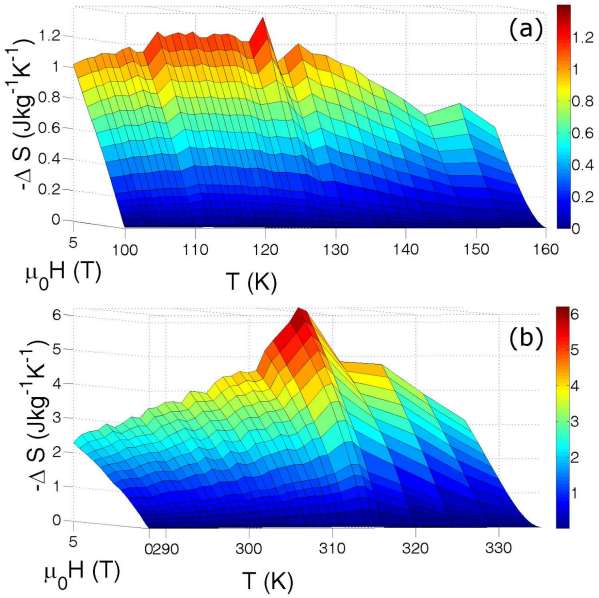

Fig. 4. Temperature dependence of the magnetic entropy change is shown in respect to magnetic fields with different magnetic flux density for (a) *as*0 sample (*Pnma*), and (b) 48*h* sample ($R\bar{3}c$).

ceramic material with the same crystal structure where the degree of JT distortion was partially released by annealing [4]. The maximal value of $-\Delta S = 6.19$ J/(kg K) ($-\Delta\mu_0 H = 5$ T, $T = 315$ K) for $a48$ sample ($R\bar{3}c$) is higher than for orthorhombic sample [4], and the value $-\Delta S = 4.08$ J/(kg K) ($\Delta\mu_0 H = 2.79$ T, $T = 315$ K, $a48$) is comparable with $-\Delta S = 5.6$ J/(kg K) ($\Delta\mu_0 H = 2.7$ T, $T = 265$ K) of a ceramic sample with the same chemical composition and $R\bar{3}c$ structure [3]. In addition $-\Delta S = 3.58$ J/(kg K) ($\Delta\mu_0 H = 2.21$ T, $T = 315$ K, $a48$) is much larger than $-\Delta S = 0.96$ J/(kg K) ($\Delta\mu_0 H = 2$ T, $T = 306$ K) of a nanosized sample with similar composition, and prepared by sol gel method [7].

Conclusions

To summary, the self combustion method in combination with heat treatment is powerful method for a preparation of magnetic nanoparticles with the Curie temperature above the room temperature, e.g., with $T_C = 315$ K and large values of the MCE with $-\Delta S = 6.19$ J/(kg K) at $\Delta\mu_0 H = 5$ T and $T = 315$ K, which have large potential for practical application. Our study underlines the dominant effect of JT distortion of the crystal lattice on magnetic properties of hole-doped manganites, which is stronger than the change of crystal structure itself.

Acknowledgments

This research was financed by projects VEGA 2/0137/19, SK-SRB-18-0066 and ITMS: 26220220186.

References

[1] A. M. Tishin, Y.I. Spichkin, *The Magnetocaloric Effect and Its Applications*, 1st ed. Institute of Physics, New York 2003.

[2] K.A. Gschneidner Jr., V.K. Pecharsky, A.O. Tsokol, *Rep. Prog. Phys.* **68,** 1479 (2005).

[3] I.K. Kamilov, A.G. Gamzatov, A.M. Aliev, A.B. Batdalov, A.A. Aliverdiev, Sh.B. Abdulvagidov, O.V. Melnikov, O.Yu. Gorbenko, A.R. Kaul, *J. Phys. D: Appl. Phys.* **40**, 4413 (2007).

[4] M. Antonak, M. Mihalik, M. Mihalik Jr., M. Zentkova, G. Gritzner, *IEEE Trans. Magn.* **50**, 6800071 (2014).

[5] A.E. Irmak, A. Coskun, E. Tasarkuyu, S. Akturk, G. Unlu, Y. Samancioglu, C. Sarikurkcu, B.M. Kaynar, A. Yucel, *J. Magn. Magn. Mater.* **322**, 945 (2010).

[6] G. Gritzner, J. Ammer, K. Kellner, V. Kavecanský, M. Mihalik, S. Matas, M. Zentkova, *Appl. Phys. A Mater. Sci. Process.* **90**, 359 (2008).

[7] A. El-Rahman, T. AboZied, A.A. Ghani, I.A. Ahmed, A. Taher, A. Salaheldin, *J. Magn. Magn. Mater.* **479**, 260 (2019).

[8] M. Zentková, M. Antoňák, M. Mihalik, M. Mihalik Jr., M. Vavra, V. Girman, M. Fitta, J. Briančin, *Low Temp. Phys.* **43**, 990 (2017).

[9] L.A. Chick, L.R. Pederson, G.D. Maupin, J.L. Bates, L.E. Thomas, G.J. Exarhos, *Matt. Lett.* **10**, 6 (1990).

[10] J. Rodriguez-Carvajal, *Physica B*, **192**, 1 (1993).

[11] V. Kusigerski, D. Markovic, V. Spasojevic, M. Tadic, M. Zentková, M. Mihalik, *Nanopart. Res.* **12**, 1299 (2010).

[12] H. Meskine, S. Satpathy, *J. Appl. Phys.* **85**, 4346 (1999).

[13] M. Antoňák, M. Mihalik, M. Zentková, M. Mihalik Jr., M. Vavra, J. Lazúrová, M. Fitta, M. Balanda, *Acta Phys. Pol. A* **126**, 296 (2014).

[14] M. Mihalik, M. Zentková, J. Briančin, M. Fitta, M. Mihalik Jr., J. Lazúrová, M. Vavra, *Acta Phys. Pol. A* **126**, 312 (2014).

[15] W. Anderson, H. Hasegawa, *Phys. Rev.* **100**, 675 (1955).